

Response to comments of Reviewers

Interactive comment on “The long-term spatio-temporal variability of sea surface temperature in the Northwest Pacific and the Near China Sea” by Zhiyuan Wu et al.

Anonymous Referee #1

Received and published: 20 Sep 2019

The authors are grateful to this reviewer for pin-point and pertinent comments and checking the paper. All comments are addressed point by point, each starting with an original comment and followed by a response in italic, as follows.

The manuscript “The long-term spatio-temporal variability of sea surface temperature in the Northwest Pacific and the Near China Sea” by Zhiyuan Wu et al., Presents the variability of the sea surface temperature (SST) in Northwest Pacific the last 164 years, on seasonal, annual and interannual scales based on monthly data sets. The analysis is well presented, and the results are interesting in terms of global warming.

***Response:** Thank you for these comments. The positive comments in our solid professional skills are good encouragement to us.*

The correlations found are mostly expected, especially between the SST and the T₂, since the temperature at 2 m and SST are strongly linked. The changes in the SST and the SSTA are closely related to El Niño 3.4. The important part of this study is the increasing SST linear trend of 0.033 °C/10 yr and especially of 0.306 °C/10 yr in the last ten years, which shows an “acceleration” in the temperature increase in the Northwest Pacific.

***Response:** We are grateful to these positive comments.*

On the other hand, it is interesting the change that the authors find in the SST around 1998. Although they do not propose an explanation for this change, it would be excellent if they tried to give some comment or proposed a hypothesis.

***Response:** Thank you for your comment. As the reviewer said, we found a very interesting phenomenon about the changes in the SST around 1998. We believe that this phenomenon has an important relationship with the El Niño, which can be confirmed in Figure 5. And the same*

phenomenon reappeared around 2016, we can understand this phenomenon from the NINO3.4 index. These discussions are in Section 3.1, lines 269 to 288 of the manuscript.

A minor issue is in Figure 12, placing a, and b on the figures to be consistent with the figure caption.

Response: *Thanks for your careful checking. We revised the Figure 12.*

The manuscript deserves to be accepted.

Response: *We are grateful to the positive comment and encouragement.*

The long-term spatio-temporal variability of sea surface temperature in the Northwest Pacific and the Near China Sea

Zhiyuan Wu^{1,2,3}, Changbo Jiang^{1,3,*}, Mack Conde⁴, Jie Chen^{1,3}, Bin Deng^{1,3}

¹ School of Hydraulic Engineering, Changsha University of Science & Technology, Changsha, 410114, China

² School for Marine Science and Technology, University of Massachusetts Dartmouth, New Bedford, MA 02744, USA

³ Key Laboratory of Water-Sediment Sciences and Water Disaster Prevention of Hunan Province, Changsha, 410114, China

⁴ School of Marine Science and Ocean Engineering, University of New Hampshire, Durham, NH 03824, USA

* Correspondence: chbjiang@csust.edu.cn

Abstract: The variability of the sea surface temperature (SST) in the Northwest Pacific has been studied on seasonal, annual and interannual scales based on the monthly datasets of ERSST 3b (1854-2017, 164 years) and OISST V2 (1988-2017, 30 years). The overall trends, spatial-temporal distribution characteristics, regional differences in seasonal trends, and seasonal differences of SST in the Northwest Pacific have been calculated over the past 164 years based on these datasets. In the past 164 years, the SST in the Northwest Pacific has been increasing linearly year by year with a trend of 0.033 °C/10 yr. The SST during the period from 1870 to 1910 is slow decreasing and staying in the range between 25.2 °C to 26.0 °C. During the period of 1910-1930, the SST as whole maintained a low value, which is at the minimum over the 164 years. The period from 1880 to 1910 is a slow decreasing trend period in the past 164 years and the SST during the 1910-1930 period was a trough of the past 164 years. After 1930, SST has continued to increase until now. The increasing trend in the past 30 years has reached 0.132 °C/10 yr and the increasing trend in the past 10 years is 0.306 °C/10 yr, which is around ten times in the past 164 years. The SST in most regions of the Northwest Pacific showed a linear increasing trend year by year, and the increasing trend in the offshore region was stronger than that in the ocean and deep-sea region. The change in trend of the SST in the Northwest Pacific shows a large seasonal difference, and the increasing trend in autumn and winter is larger than that in spring and summer. There are some correlations between the SST and some climate indexes and atmospheric parameters, the correlation between the SST and some atmospheric parameters have been discussed, such as NAO, PDO, SOI anomaly, TCW, Nino 3.4, SLP, Precipitation, T2 and wind speed. The lowest SST in the Near China Sea basically occurred in February and the highest in August. The SST fluctuation in the Bohai Sea and Yellow Sea (BYS) is the largest with a range from 5 °C to 22 °C, the SST in the East China Sea (ECS) is from 18 °C to 27 °C, the smallest fluctuations occurs in the South China Sea (SCS) maintained at range of 26 °C to 29 °C. There are large differences between the mean and standard deviation in different sea regions.

37 **Keywords:** sea surface temperature; spatio-temporal distribution; interannual and interdecadal time
38 scales; the Northwest Pacific

39 1. Introduction

40 The ocean is one of the important components of the ocean-atmosphere coupling system (Chelton
41 and Xie, 2010; Wu et al., 2019a,b). Relative to the atmosphere, the ocean has characteristics such as slow
42 change and large heat capacity (England et al., 2014). Because of the gradual changes in the ocean, climate
43 change at the interannual, decadal, and longer timescales may be closely related to the ocean (Trenberth
44 and Hurrell, 1994; Ault et al., 2009). The Sea Surface Temperature (SST) is the basis for the interaction
45 between the ocean and the atmosphere (Wu et al., 2019c,d), and it characterizes the combined results of
46 ocean heat content (Buckley et al., 2014; Griffies et al., 2015), dynamic processes (Takakura et al., 2018).
47 It is a very important parameter for climate change and ocean dynamics process, reflects sea-air heat and
48 water vapor exchange. Observations and numerical simulations show that large-scale sea surface
49 temperature anomalies of over 20° in longitude and latitude can cause significant changes in atmospheric
50 circulation, such as the El Niño and La Niña phenomena (Chen et al., 2016; Zheng et al., 2016). During
51 El Nino, the trade winds in the tropical East Pacific will be weakened, and the SST increased significantly,
52 which was 3~5°C higher than normal years. As a result, major changes have been made in the
53 atmospheric circulation and ocean circulation, which has caused the worldwide atmospheric and marine
54 environment and the abnormality of climate (Li et al., 2017).

55 The Northwest Pacific is particularly affected by the El Niño in the East Pacific and determines the
56 oceanic climate change in China (Hu et al., 2018). On one hand, climate change causes an increasing SST
57 in the northwestern Pacific, which increases the vertical stratification of the water, affects the atmospheric
58 circulation, and changes the intensity and period of coastal winds and upwelling. On the other hand, the
59 10-year periods Pacific Decadal Oscillation (PDO) and the El Niño-Southern Oscillation (ENSO) occur
60 on average every 2 to 7 years, resulting in large variations in upwelling (Xiao et al., 2015; Yang et al.,
61 2017; Xue et al., 2018). These factors will all lead to the impact on the marine environment in Chinese
62 coastal areas, causing land-based droughts, ~~and~~ floods and climate disasters (Xu et al., 2018). Therefore,
63 it is very urgent to study the impact of climate change on SST in the Northwest Pacific and the Near China
64 Sea. As one of the main parameters of global climate change and one of the important characterizations
65 and predictors of El Niño, the study of SST changes is particularly important.

66 Previous scholars have done a lot of work on the changing trend of SST. According to the Fifth
67 Assessment Report (AR5) of the Intergovernmental Panel on Climate Change (IPCC), the global SST
68 warming trend was 0.064 °C/10 yr between 1880 and 2012 (Pachauri et al, 2014). In fact, many studies
69 have shown that the Pacific SST anomalous changes are closely related to global and regional climate
70 changes, and it has multi-scale temporal variations (Graham, 1994; Latif, 2006; Shakun and Shaman, 2009;
71 Li et al, 2014). In addition, the El Niño-Southern Oscillation (ENSO) and the Pacific Decadal Oscillation
72 (PDO), which are closely linked to global and regional climate change, are found in this area. Therefore,
73 the Pacific is one of the key ocean areas that scholars have studied for a long time (Bao and Ren, 2014;
74 Mei et al., 2015; Stuecker et al, 2015; Wills et al, 2018).

75 So far, two types of main meteorological SST datasets have been obtained: one based on measured
76 mid-resolution (1° - 5°) 100-year datasets and the other based on satellite high-resolution (1-10km) decade
77 datasets (Wang et al., 2011; Smith et al., 2014; Huang et al., 2015, 2016; Diamond et al., 2015). The former
78 has rebuilt a time series of months over 150 years and the latter has accumulated over 30 years of time
79 series on a daily average basis (Tian et al., 2019). The existing climatic datasets already have conditions
80 for allowing the creation of a natural mode of change in SST in terms of duration and resolution (Liu et
81 al., 2017; Wang et al., 2018). With the continuous improvement of ocean observation technology and the
82 accumulation of satellite remote sensing data, the conditions for the scholars use the satellite data for short-
83 term climate change research have been met. In recent years, the research and discussion on the interannual
84 change of SST based on satellite remote sensing SST has attracted wide attention (Tang et al., 2003; Yang
85 et al., 2013; Zhang et al., 2015; Skirving et al., 2018).

86 Satellite remote sensing can achieve large-area simultaneous measurements with high temporal and
87 spatial resolution. The remote sensing SST obtained is conducive to a more comprehensive and rapid
88 understanding of oceanographic phenomena that affect the ocean surface, including El Niño (Robinson,
89 2016). At present, about 30 years of satellite remote sensing SST data have been accumulated (Franch et
90 al., 2017), and a set of sea surface temperature data has been provided to study the conditions for the
91 occurrence and development of ocean surface heat change modes in the temporal and spatial span and
92 resolution. So, satellite remote sensing SST has received widespread attention in recent years.

93 At present, based on satellite remote sensing data, the time scales for the study of changes in SST in
94 the Northwest Pacific, especially in the Near China Sea, are mostly within 20 years, which is relatively
95 short for studying climate change (Song et al., 2018; Pan et al., 2018). Most of the ~~space~~-research is
96 targeted at specific local sea areas, and there is less research on the changes of the SST in the Northwest
97 Pacific covering all marginal seas of China. Therefore, it is necessary to study the SST variation of large-
98 scale and long-term sequences based on satellite remote sensing data.

99 Previous scholars have made great contributions to the study of global warming, but most of them
100 are the overall changes in the regional average SST, and they tend to ignore the characteristics of changes
101 in certain key sea areas. There are great differences in the trends of SST in different sea areas. The long-
102 term trend of the SST changes in the Northwest Pacific (0° N- 60° N, 100° E- 180° E) over the past 164
103 years (1854-2017) have been calculated based on the monthly datasets of ERSST 3b in this study. The
104 temporal and spatial distribution characteristics of SST, the overall long-term sequence variation trend,
105 the regional variation of the seasonal trend, and the seasonal differences were analyzed. The correlations
106 with SST changes and climate parameters and indexes are been analyzed. To provide a reference for the
107 study of global climate change, the characteristics of SST changes in the Near China Sea has been studied
108 in this paper.

109 High spatial resolution SST datasets including average SST field and monthly SSTA field are been
110 obtained. In view of the fact that there are many interannual and intra-annual changes, this paper analyzes
111 the characteristics of SST changes based on these datasets. The trend, inter-decadal changes in SST and
112 their causes, and the correlation with the climate parameters and indexes such as Nino-3.4 index are
113 relatively low. The ocean thermal dynamic phenomenon is preliminarilly discussed. The datasets are

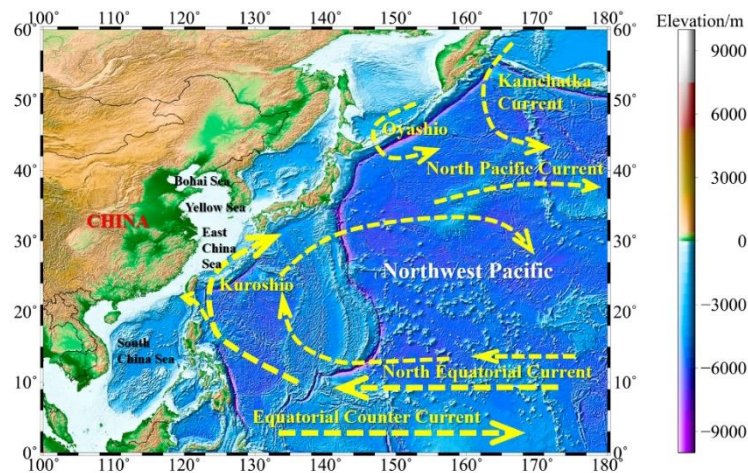
114 processed and analyzed to study the trend changes of the SST in the Northwest Pacific. To explore the
115 correlation and response mechanisms with climate systems such as the ENSO and the PDO, and to conduct
116 a detailed analysis of typical sea areas.

117 2. Study region, Data and Methods

118 2.1. Study Region

119 The Northwest Pacific is the northwest region of the Pacific, ~~are is~~ defined as the offshore region of
120 0°N- 60°N and 100°E - 180°E in this study (Fig.1). There are more tropical cyclones over the Northwest
121 Pacific than any other sea area in the world, with an average annual average of 35. About 80% of these
122 tropical cyclones will develop into typhoons. On average, about 26 tropical cyclones per year reach at least
123 the intensity of tropical storms, accounting for about 31% of the global tropical storms, and more than
124 double the number of any other area. The sea-air interaction in this area is very strong and the change of
125 SST is worth to explore.

126
127



128 **Figure 1.** Bathymetric map of the Northwest Pacific and ocean circulation.

128 2.2. SST Dataset

129 Several data sources are used to analyze the long-term temporal and spatial variability of SST in the
130 Northwest Pacific in this present study. Long-term statistics are based on the monthly SST data from the
131 Extended Reconstructed Sea Surface Temperature (ERSST) 3b (1854-2017) (Smith et al., 2008). The
132 ERSST dataset is a global monthly sea surface temperature analysis derived from the International
133 Comprehensive Ocean–Atmosphere Dataset with missing data filled in by statistical methods. This
134 monthly analysis begins in January 1854 continuing to the present (<https://www1.ncdc.noaa.gov/pub/data/cmb/ersst/v3b/>). The primary SST dataset analyzed in this study is the NOAA Optimum
135 Interpolation (OI) Sea Surface Temperature (SST) V2 (OISST V2 1982-2017, <http://www.esrl.noaa.gov/psd/data/gridded/data.noaa.oisst.v2.html>) (Reynolds et al., 2002, 2007). There are many of SST data sets, such as the HadISST1 data set replaces the GISST data sets, and is a unique combination of monthly globally-complete fields of SST and sea ice Concentration on a 1 degree latitude-longitude grid from 1870 to date. But, from May 2007 the data set of in situ measurements used in HadISST has changed. The

140

141 advantage of this dataset is apparent when compared with other gridded datasets such as HadISST, ERSST
142 and OSTIA, which spans only the period since 2007.

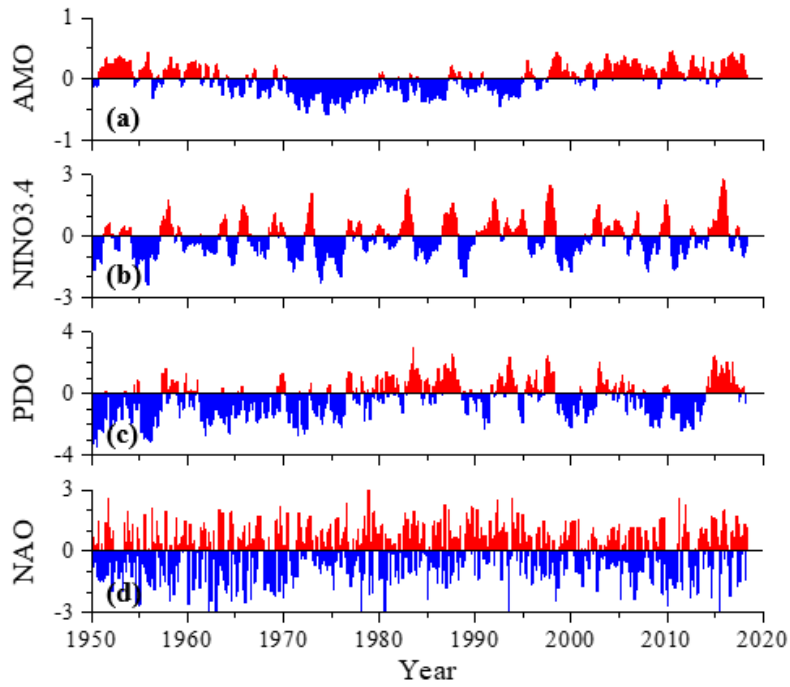
143 The seasonal mean data are obtained by averaging the monthly average SST after the above-
144 mentioned processing. The spring is March, April and May (MAM), the summer is June, July and August
145 (JJA), the autumn is September, October and November (SON), and the winter is December of the
146 previous year and January and February (DJF).

147 The SST anomaly is the deviation from the long-term SST average of the observations of the SST
148 describing a particular area and time. The year anomaly represents the deviation of the average of the SST
149 for a given year from the mean of the multi-year SST. The month anomaly represents the deviation of the
150 average of the SST for a particular month from the average of the SST for that particular month for many
151 years. In this paper, the mean value from 1854 to 2017 is taken as the climate mean state, and the sea
152 surface temperature anomaly is subtracted from the SST field to obtain the SSTA field.

153 *2.3. Climate Index Dataset*

154 The Atlantic Multidecadal Oscillation (AMO) is a climate cycle that affects the sea surface
155 temperature (SST) of the North Atlantic Ocean based on different modes on multidecadal timescales
156 (<http://www.esrl.noaa.gov/psd/data/timeseries/AMO>, McCarthy et al, 2015). Niño 3.4 index uses SST to
157 characterize ENSO, the Niño 3.4 SST region consists of temperature measurements from between 5° N -
158 5° S and 120° - 170° W (Gergis and Fowler, 2005). The PDO index is the time coefficient of the first mode
159 obtained by performing EOF of the mean SSTA ~~in~~to the north of 20° N in the North Pacific
160 (<http://jisao.washington.edu/pdo/PDO.latest>). The North Atlantic Oscillation (NAO) is the most
161 prominent modality in the North Atlantic. Its climate impact is most prominent mainly in North America
162 and Europe, but it may also have an impact on the climate in other regions such as Asia. Recent studies
163 have not only further confirmed its existence, but also revealed its connection with a wide range of oceans
164 and atmospheric conditions.

165 The correlation between the SST and the atmospheric parameters is analyzed based on the ERA-
166 Interim data. ERA-Interim refers to the European Centre for Medium-Range Weather Forecasts (ECMWF),
167 which is an independent intergovernmental organization supported by 34 countries. Its goal is to develop
168 numerical methods for ~~mid-term mesoscale~~ weather forecasting. The country provides forecasting services,
169 conducts scientific and technological research to accumulate forecasts, and accumulates meteorological
170 data. ERA-Interim is the latest global reanalysis product developed by ECMWF. The weather data and
171 climate data from January 1988 to December 2017 are used in this paper, such as sea surface temperature,
172 sea-to-air interface heat flux, and wind field data at a height of 10m, the spatial resolution of these datasets
173 is 1.5°×1.5°.



174
175
176

Figure 2. AMO index (a), Niño 3.4 index (b), PDO index (c) and NAO index (d) during 1950~2017.

177 *2.4. Methods*

178 Regression analysis is an important part of mathematical statistics and multivariate statistics. It is a
179 mathematical method to study the correlation between variables and variables. The regression analysis has
180 a wide range of applications in the statistical forecasting of oceans and atmospheres. It is used to analyze
181 the statistical relationship between a variable (called forecast) and one or more independent variables
182 (called predict), and to establish a forecast. The regression equation produced by the quantity and forecast
183 factor, and then based on this equation to make predictions of the forecast volume. Regression analysis
184 includes linear regression and nonlinear regression. The linear regression is commonly used, and a linear
185 regression analysis method is used in this paper.

186 Use x_i to represent a climate variable with a sample size of n . Use t_i to represent the time
187 corresponding to x_i and establish a linear regression between x_i and t_i . The formula can be expressed as:

$$x_i = a + bt_i, \quad i = 1, 2, 3, \dots, n \quad (1)$$

188 Where, a is the regression constant and b is the regression coefficient. a and b can be calculated using
189 the least squares method.

190 For the observation data x_i and the corresponding time t_i , the least-squares calculation result of the
191 regression coefficient b and the constant a is expressed as:

$$b = \frac{\sum_{i=1}^n (x_i - \bar{x})(t_i - \bar{t})}{\sum_{i=1}^n (x_i - \bar{x})^2} \quad (2)$$

$$a = \bar{x} - b\bar{t}$$

192 The correlation coefficient between time t_i and x_i is:

$$r = \frac{\sqrt{\sum_{i=1}^n t_i^2 - \frac{1}{n} \left(\sum_{i=1}^n t_i \right)^2}}{\sqrt{\sum_{i=1}^n x_i^2 - \frac{1}{n} \left(\sum_{i=1}^n x_i \right)^2}} \quad (3)$$

193 The correlation coefficient r is expressed as the degree of closeness of the linear correlation between
 194 the variable x and the time t . When $r > 0$, $b > 0$, indicating that x increases with time t ; when $r < 0$, $b < 0$,
 195 indicating that the variable x decreases with time t . ~~A significance test is performed~~ ~~Perform a significant~~
 196 ~~test~~ on the correlation coefficient to determine the significance level α (confidence is $1 - \alpha$) first. If
 197 $|r| > r_\alpha$, shows that the trend of the variable x with time t is significant, otherwise it is not significant.

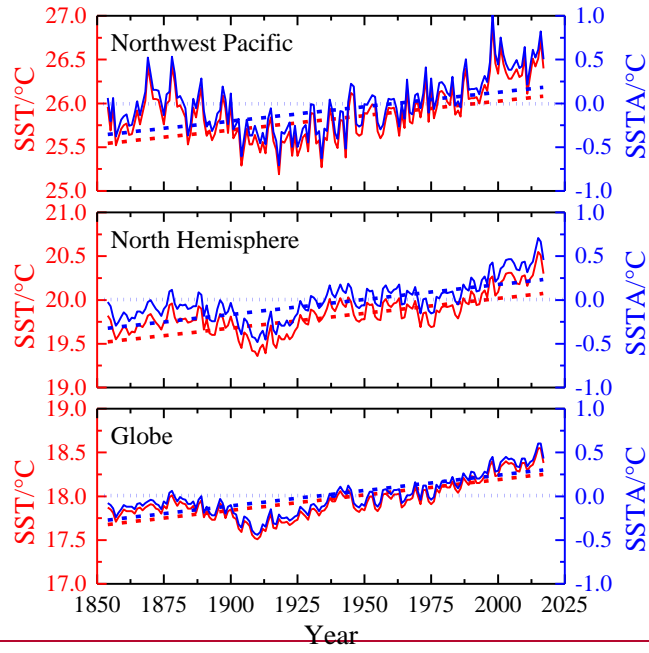
198 3. Results and Discusses

199 3.1. Temporal distribution of SST

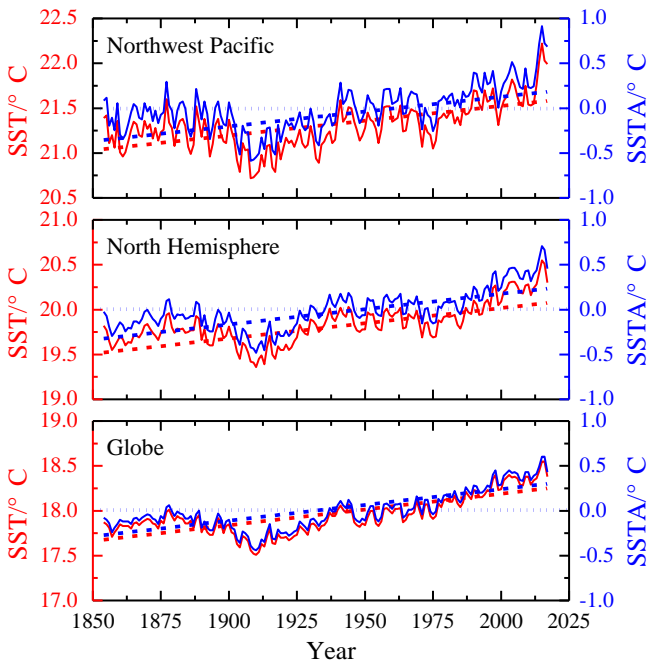
200 With the gradual warming of the global climate, the average temperature of the ocean is also rising.
 201 In order to reflect the overall trend of SST in the Northwest Pacific over the past 164 years (1854-2017),
 202 the average monthly SST data from 1854 to 2017 was used. The time series curve of SST in the Northwest
 203 Pacific, the Northern Hemisphere, and the global ocean was obtained by processing, and the overall trend
 204 of the SST was analyzed, as shown in Fig. 3. As can be seen from the figure, SST in the different region
 205 have shown an increasing trend and SST has shown a significant increasing trend since the 20th century.

206 The SST datasets were used to calculate the SST anomaly time series and its linear variation trend in
 207 the Northwest Pacific, the Northern Hemisphere and the global ocean as shown in Fig. 3. The slope of the
 208 linear equation with one unknown obtained by least-squares fitting is the annual change rate of SST, as
 209 shown in Table 1. It shows the increasing trend of SST at different time scales. It can be seen that the data
 210 shows that the SST in the different region has shown a significant warming trend as a whole. It can be
 211 seen from Table 1 that from 1854 to 2017, the SST trend of Northwest Pacific, North Hemisphere and
 212 global ocean has increased by 0.033 °C to 0.035 °C per 10 years. In the past 50 years, the increasing rate
 213 of SST has reached 0.10 °C/10 yr or more, and the increasing rate in the last 10 years has reached 0.30°C.
 214 It can be seen that the warming trend of SST in the Northwest Pacific is very significant.

215



216



217

Figure 3. The temporal variability of annual SST.

218

Table 1. The average trend of SST (Unit: °C/10 yr).

	NWP	NH	GLO
1854-2017 (164yr)	0.033	0.034	0.035
1918-2017 (100yr)	0.100	0.059	0.069
1968-2017 (50yr)	0.128	0.128	0.102
1988-2017 (30yr)	0.132	0.149	0.102
2008-2017 (10yr)	0.306	0.379	0.274

219 NWP: Northwest Pacific; NH: North Hemisphere; GLO: Globe. All the trend ~~is~~ are significant
220 at the 95% confidence level.

221 There exist decadal to multi-decadal variations in the SST and SST anomalies series, with a general
222 cool period from the 1880s to 1910s, a weak warm period from 1920s to 1940s, a weak cool period from
223 1970s to 1980s, and a recent warm period from 1990s to present. Fig.3 also show that the interannual to
224 decadal variability is larger in the North Western Pacific, and it is smaller in the global ocean, indicating
225 an increase in SST anomaly variability with the area. It is also interesting to note that the latest 10 years
226 see a larger increasing trend of annual mean SST than that for the last 164 years, 100 years, 50 years and
227 30 years, indicating an obvious speed-up of warming of the Northwest Pacific, North Hemisphere and
228 globe ocean occurs in the last 10 years, and the growth rate over the past decade has been around ten times
229 that of the past 164 years.

230 In the past 164 years, the correlation coefficient of SST trends in the Northwest Pacific was 0.73. It
231 passed the 95% ~~significancereliability~~ test, which shows that the linear trend is significant, and the
232 regression coefficient is 0.0033. This shows that in the past 164 years, the SST in the Northwest Pacific
233 has been increasing linearly year by year at a rate of 0.033 °C/10 yr. It can be seen from Fig. 3 that during
234 the period of 1870-1910, ~~the SST it showed a slowly decreasing trended, SST basically fluctuates~~
235 ~~slightly staying in the range~~ between 25.2 °C to 26.0 °C; during the period of 1910-1930, the SST as
236 whole maintained a low value, and the change range was small, which is at the minimum valley of
237 nearly over the 164 years; ~~and the curve trend is also very gentle; after since~~ 1930, the SST ~~oscillated~~
238 gradually, has started to rise with oscillation and the trend has continued to this day.

239 In order to demonstrate the seasonal variation of the SST trend in the Northwest Pacific, the SST at
240 1°×1° at each grid point in the Northwest Pacific was averaged from 1854 to 2017 by winter, spring,
241 summer, autumn and year in this study. The season-by-season linear trend of SST at each grid point has
242 been analyzed. At the same time, the season-by-season time series of the SST anomalies were being
243 calculated and the seasonal variation of the comparison trends was shown in Fig 4.

244 Fig.4 (a) and (b) show seasonal and annual mean SST and SST anomalies series. The blue lines are
245 their trends of every seasonal mean SST and SST anomalies series for the Western Pacific during 1854-
246 2017, the red lines ~~is~~ are their trends during 1988-2017. The increasing trends during 1854-2017 is between
247 0.032 °C/10 yr and 0.035 °C/10 yr for all seasons. The seasonal pattern for the latest 30 years shows a
248 more significant warming trend than that over the 164 year period. The same as the annual pattern, seasonal
249 pattern for the latest 30 years shows more significant warming trend than 164 years. Significant warming
250 occurs in all seasons with those of autumn and winter being the largest, reaching 0.146 °C/10 yr and
251 0.124 °C/10 yr respectively at the last 30 years, and that of spring the smallest.

252 An El Niño or La Niña event is identified if the NINO3.4 index exceeds +0.4°C for El Niño or -0.4°C
253 for La Niña, so ±0.4 °C is used for discriminating anomalies in this study. The magenta points mean the
254 SST anomaly larger than 0.4 °C, and the cyan points mean the SST anomaly is smaller than -0.4 °C in the
255 Fig.4 (b). As can be seen from the figure, during the period from 1890 to 1960, there were more negative
256 anomalies and less than -0.4 °C, indicating that there was a cool period during this period. In the period

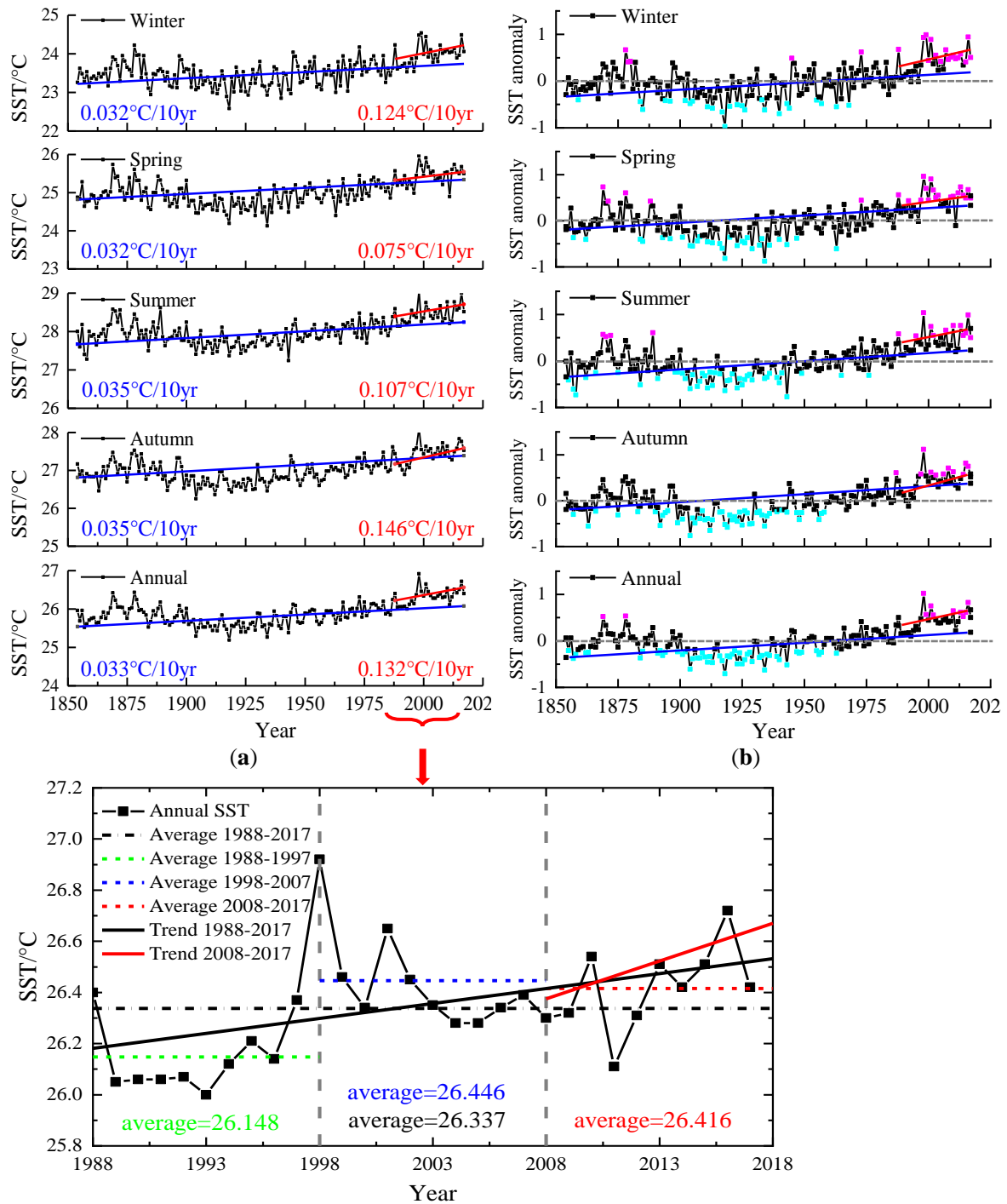
257 from 1988 to 2017, there are more positive anomalies and more than 0.4 °C, indicating that there is a warm
258 period in the past 30 years.

259 In the analysis of the SST changes in the Northwest Pacific during the past 164 years, it has been
260 found that there was a strong warming trend in SST over the past 30 years since 1988. It had been shown
261 that the SST in the Northwest Pacific has an overall warming trend since the 1970s in the previous studies
262 (Zhou et al., 2009; Kosaka et al., 2013) and this study. The time series ~~curve~~ of the SST in the Northwest
263 Pacific from 1988 to 2017 was plotted as shown in Fig. 4(c).

264 Yamamoto's (1986) method has been used to determine the ~~extremummutation~~ point, and the formula
265 is:

$$R_{SN} = \frac{|\overline{X_1} - \overline{X_2}|}{S_1 + S_2} \quad (4)$$

266 Where, $\overline{X_1}$, $\overline{X_2}$, S_1 , S_2 are the average and standard deviation of the two stages before and after
267 the ~~extrememutation~~ year. It was found that there were six stations when $X_1 = X_2 = 10$, $R_{SN} \geq 0.7$ in 10 years
268 before and after 1998/1999, and the significance level of the statistic reached $\alpha = 0.05$, according to which
269 the SST was considered to have a ~~extremummutation~~ in this year. The difference between the mean value
270 of the anomaly before and after the ~~extrememutation~~ was 0.30°C, and the similar results can also be seen
271 in Fig. 4(c). It can be found that in the past 30 years, the SST in the Northwest Pacific has significantly
272 warmed up as a whole. The highest annual mean SST appears in 1998, and the temperature undergoes a
273 weak decreasing trend since then, but the average SST during 1998-2007 reaches 26.446 °C, which is
274 higher than around 0.3 °C during 1988-1997. In the last 30 years of SST in the Northwest Pacific, the
275 increasing trend in the last 10 years is obviously greater than the trend in the last 30 years.



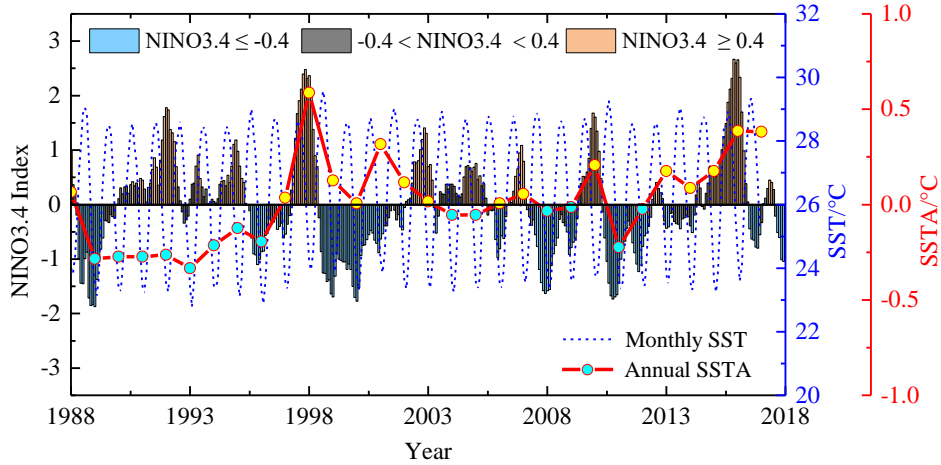
276
277
278
279

Figure 4. Variability of seasonal/annual SST. (a) the annual SST over the 1854-2017 period; (b) the SST anomaly over the 1854-2017 period; (c) the SST over the 1988-2017 period (the latest 30 years).

280
281
282
283
284

The monthly average sea surface temperature in the Northwest Pacific is represented by an undulating curve, as shown in the blue dashed line in Fig. 5, and the sea surface temperature anomaly is a red dotted line. The positive value is filled in yellow, and the negative value is filled in cyan. The NINO3.4 index is one of several El Niño/Southern Oscillation (ENSO) indicators based on sea surface temperatures. NINO3.4 is the average sea surface temperature anomaly in the region bounded by 5°N to 5°S, from

285 170°W to 120°W. This region has large variability on El Niño time scales, and is close to the region where
 286 changes in local sea surface temperature are important for shifting the large region of rainfall typically
 287 located in the far western Pacific. An El Niño or La Niña event is identified if the 5-month running-average
 288 of the NINO3.4 index exceeds +0.4°C for El Niño or -0.4°C for La Niña for at least 6 consecutive months.



289
 290 **Figure 5.** The Nino 3.4 index and SST/SSTA during 1988 to 2017. (El Niño in pink and La
 291 Niña in blue.).

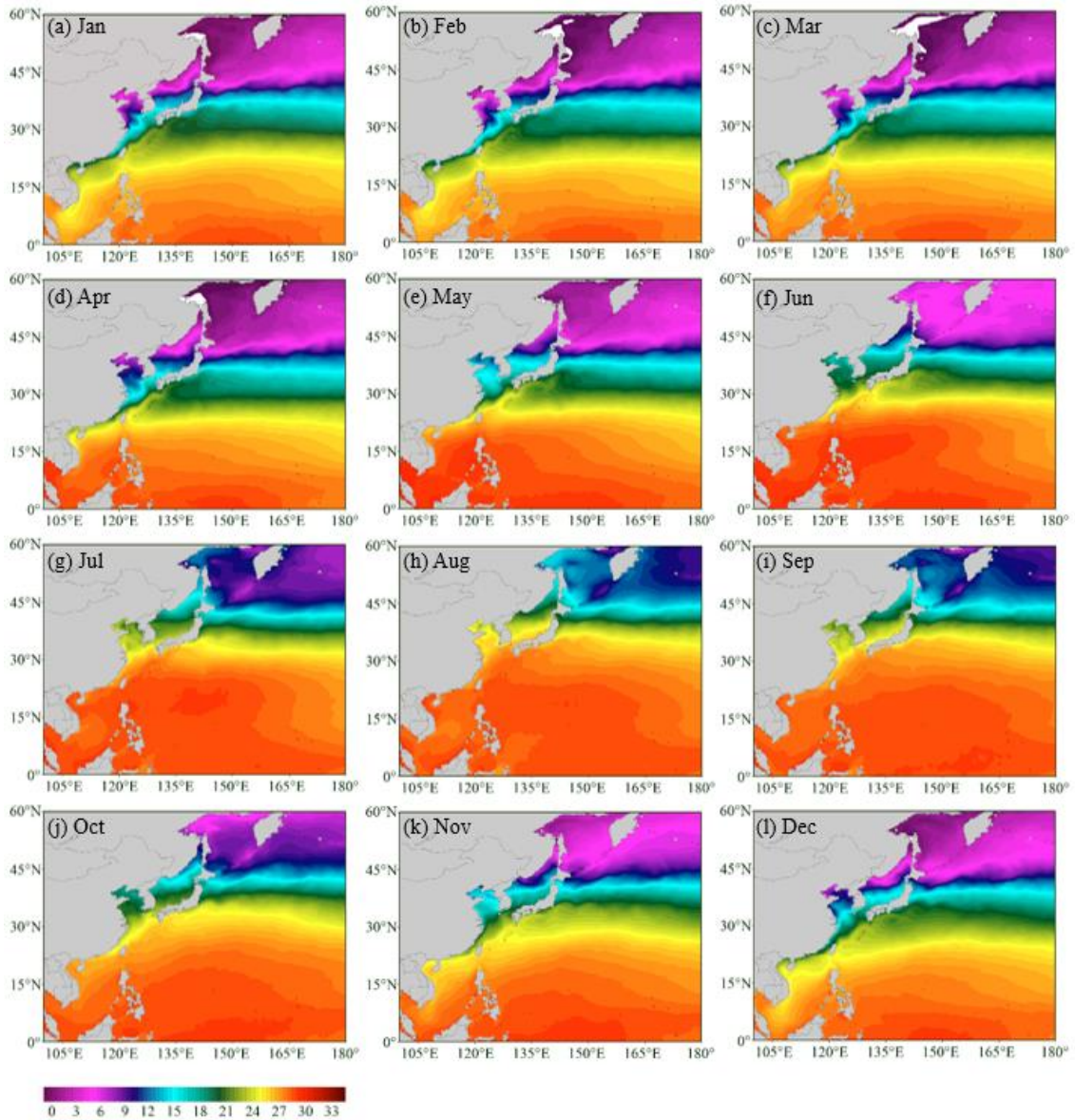
292 It can be seen from Fig.5 that the SSTA minimum value point occurs in 1989 to 1996; the maximum
 293 value point occurs in 1998 and 2016, and the maximum year coincides with the El Niño year. It is shown
 294 that the anomalous changes of the SST in the Northwest Pacific are closely related to the occurrence year
 295 of ENSO. The changes of the SST in the Northwest Pacific are obviously affected by the anomalous
 296 changes of SST in the Equatorial Pacific. The average SSTA was basically negative before 1996, and the
 297 basic value after it was positive. That is, the average SSTA was generally lower than the average of 1988-
 298 2017 before 1996, and the average SSTA after 1996 was basically higher than the average of 1988-2017,
 299 which is also reflected in Fig. 4(c).

300 In the low-latitude region, SST is more evenly distributed along the latitudes in January to April and
 301 November to December, and are higher in the south and lower in the north. From May to October, the
 302 distribution of SST along the latitude is tilted, showing the distribution characteristics of higher in the
 303 southwest and lower in the northeast, which is affected by the ocean circulation. In addition, as can also
 304 be seen in Fig. 6, in the low-latitude region, the SST range of change in different months is relatively small,
 305 between 27 °C to 33 °C, the change range of 5 °C to 6 °C. In the high-latitude region, the SST can be less
 306 than 3 °C at the lowest, and greater than 15°C at the highest, with a relatively large variation of more than
 307 12 °C.

308 3.2. Spatial distribution of SST

309 Fig. 6 shows the spatial distribution of the 30-year average SST for each month of 1988-2017. From
 310 the figure, we can find that the spatial distribution of annual average SST in each month is similar, and the
 311 SST is higher in the low-latitude (near equator) region and lower in the high-latitude region. In low-latitude
 312 region, SST is more evenly distributed along the latitudes in January to April and November to December,

313 and are higher in the south and lower in the north. From May to October, the distribution of SST along the
 314 latitude is tilted, showing the distribution characteristics of higher in the southwest and lower in the
 315 northeast, which is affected by the ocean circulation. In addition, as can also be seen in Fig. 6, in the low-
 316 latitude region, the SST range of change in different months is relatively small, between 27 °C to 33 °C,
 317 the change range of 5 °C to 6 °C. In the high-latitude region, the SST can be less than 3 °C at the lowest,
 318 and greater than 15°C at the highest, with a relatively large variation of more than 12 °C.



319

320

Figure 6. Spatial distribution of monthly SST over the 1988-2017 period.

321

322

323

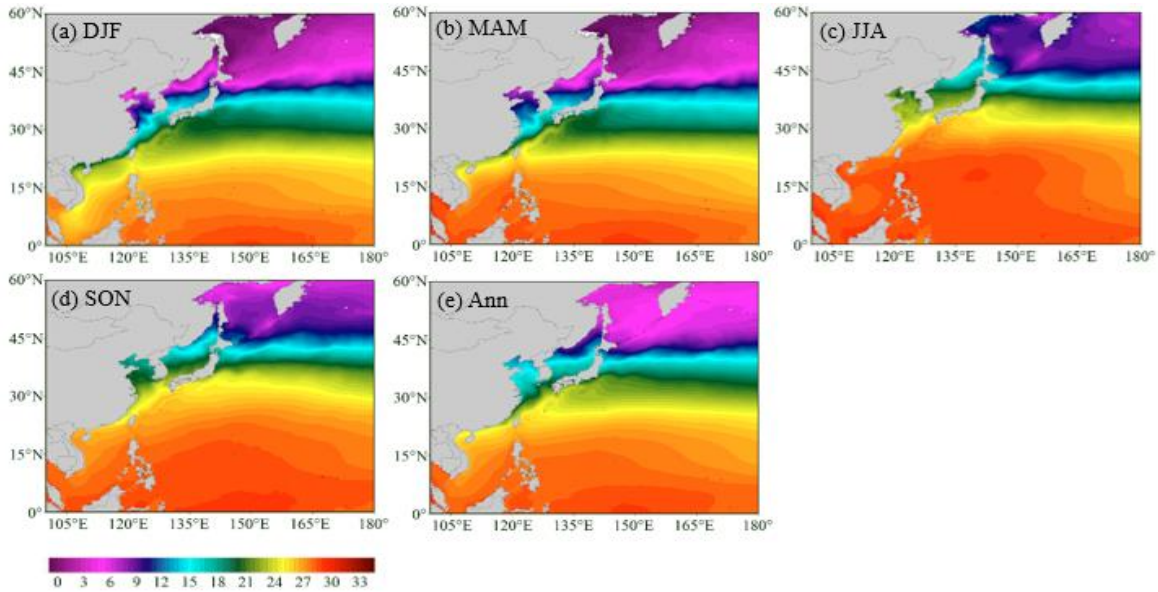
324

325

326

Fig.7 shows the spatial distribution of seasonal and annual mean SST during the 1988-2017 period. As can be seen from the figure, the spatial distribution of average SST in each season and annual is similar, and similar to the monthly results (Fig. 6). In the low-latitude region, the SST is higher, but in the high latitudes. SST is relatively low. Annual mean SST decreases with increasing latitude, with high temperature ranging from 26°C to 28°C in the south and low temperature ranging from 3°C to 6°C in the north, which is closely related to the solar radiation distribution in the deep-sea region. The isotherm is

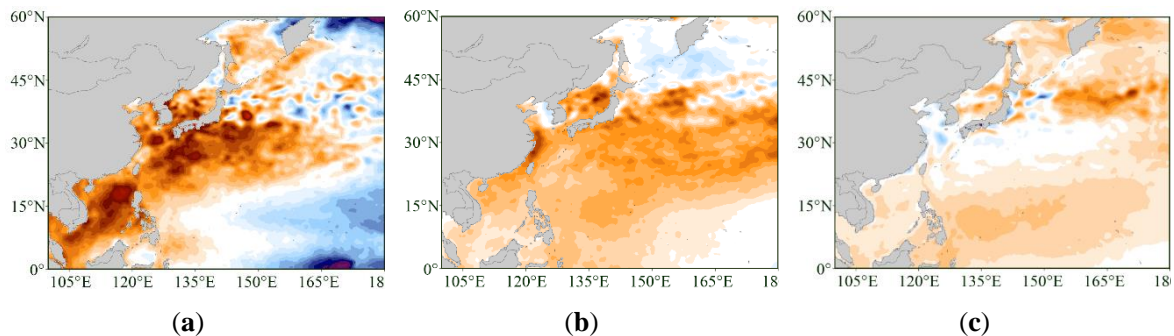
327 northeast–southwest oriented and the SST gradient increases as getting closer to the mainland coastal line.
 328 It is obvious that the landmass effect in the winter time has contributed to the tilting of the isotherms,
 329 which was pointed out by Bao et al (2014).



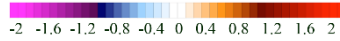
330
 331 **Figure 7.** Spatial distribution of seasonal/annual SST over the 1988-2017 period (a) Winter:
 332 DJF; (b) Spring: MAM; (c) Summer: JJA; (d) Autumn: SON (e) Annual.

333 Fig. 8 shows the results of SST anomaly in three characteristic stages. Fig. 8(a) shows the SST
 334 anomaly for the annual 1998 minus 1988-2017, Fig.8 (b) is the annual SST difference between the 10
 335 years after 1998 (1998-2007) and the previous 10 years (1988-1997) and Fig.8 (c) is the SST anomaly for
 336 the last 10 years (2008-2017) and the past 30 years (1988-2017).

337 It can be seen that there was a significant positive anomaly across the past 30-year average in 1998
 338 from Fig. 8(a). The positive anomalies around 1.0°C are shown in a large area in the Near China Sea,
 339 indicating that the SST is significantly warmer. In the southeast and northeast of the Northwest Pacific,
 340 negative anomalies have occurred in this region, and the lowest is close to -0.6°C, indicating that the SST
 341 has cooled in this region. The SSTa in the Northwest Pacific showed a trend of high in the west and low
 342 in the east. From the previous analysis, we found that this extremummutation is highly coincident with El
 343 Niño (Fig. 5). Therefore, it is likely that this phenomenon has been caused by the temperature difference
 344 and time difference caused by the transfer of high-temperature water in the Northeast Pacific to the
 345 Northwest Pacific under the combined influence of atmospheric circulation and ocean circulation.



346



347

Figure 8. (a) Ann 1998 minus 1988-2017; (b) Ann 1998-2007 minus 1988-1997; (c) Ann 2008-2017 minus 1988-2017.

348

349

It can be seen from Fig. 8(b) that the SST during the 10 years from 1998 to 2007 has significantly increased compared with the previous 10 years from 1988 to 1997. The positive anomaly occurs to be 0.4°C to 0.8°C in the south region of 40° N. In the 10 years since 1998, the SST in the region has increased by 0.4°C to 0.8°C over the previous 10 years. In the region between 45° N and 60° N, the effect is small and is maintained between -0.2°C and 0°C, indicating that the SST in this region has not changed substantially or slightly.

350

351

352

353

354

355

356

357

358

359

360

361

Fig. 8(c) shows the anomalous results of SST over the last 10 years (2008-2017) and relatively nearly 30 years (1988-2017). As can be seen from the figure, in addition to the Bohai Sea, the Yellow Sea, and the southern region of Japan, there is a wide range of positive anomaly in other regions, and the past 10 years have increased on average in the past 30 years. From Fig. 4(a) and (b), we have known that the increasing trend of SST over the past 30 years is around three to four times that of the rising trend of SST over the past 164 years. Therefore, the increasing trend of SST in the past 10 years is more significant, which is consistent with the results in Fig. 4(c) and Table 1.

362

3.3. Correlation between the SST and the atmospheric parameters

363

364

365

366

367

368

369

370

371

372

Based on monthly data from ERA-Interim, there is some correlation between SST and atmospheric parameters have been shown in Fig.9, all marked patterns are at the level of significance equal to 0.05. It can be seen from Fig. 9(a) that there is a non-significant correlation between SST and North Atlantic Oscillation (NAO), but in the South China Sea and around the region. It shows a weak negative correlation between South China Sea SST and NAO. The Pacific Decadal Oscillation (PDO) is an important factor of climate change of the Northwest Pacific, and it has a strong correlation with ENSO. The PDO has a great influence on the Asian monsoon and climate change in the Northwest Pacific and is closely related to ENSO. There is a significant negative correlation between SST and PDO can be seen from Fig. 9(b). The Niño-3.4 index is usually used to indicate the intensity of the El Niño/La Niña event. So there is a significant negative correlation between SST and the atmospheric parameters Nino 3.4 in Fig. 9(d).

373

374

375

376

377

378

379

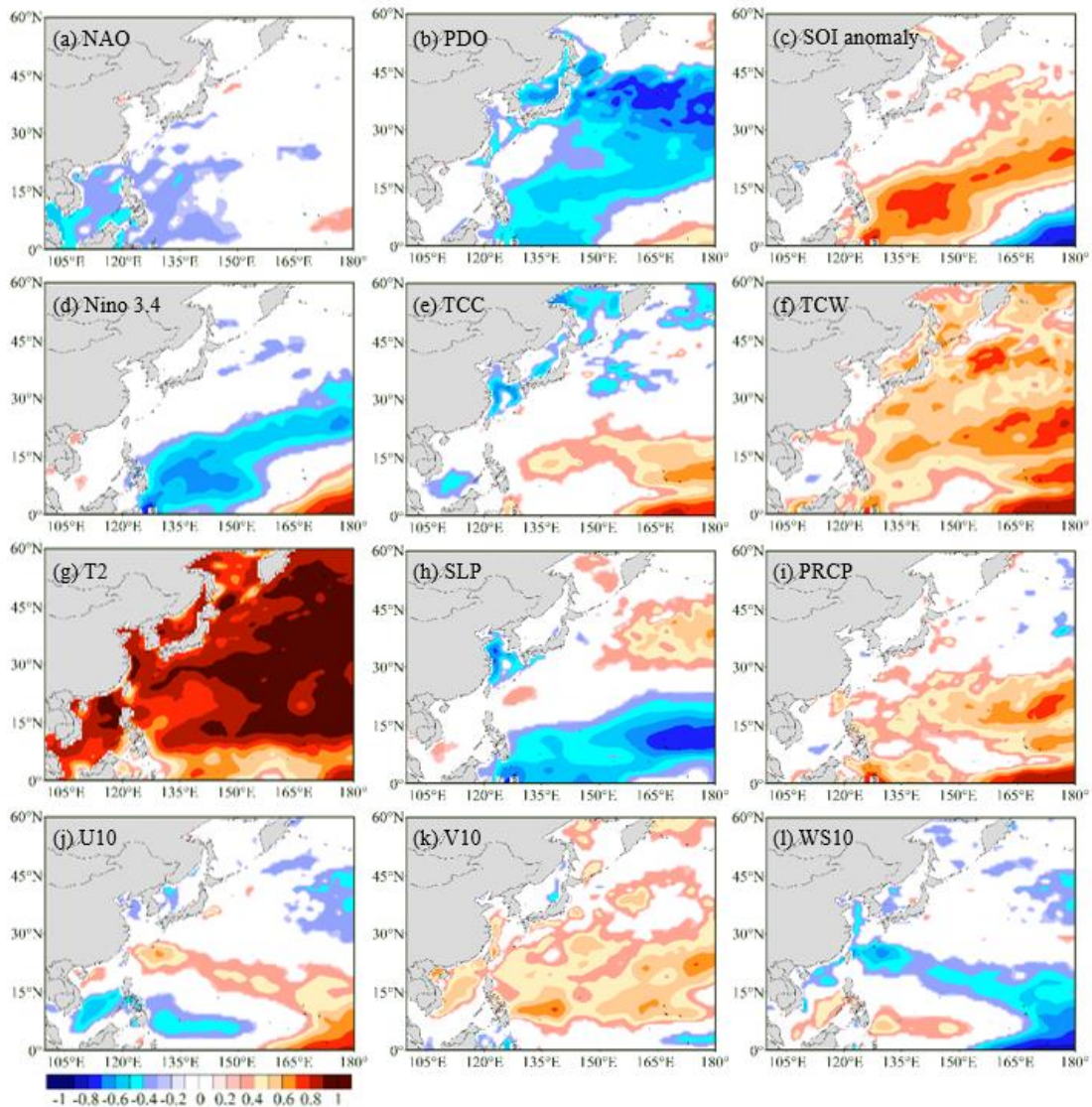
There is a significant positive correlation between SST and the Southern Oscillation Index (SOI) in Fig. 9(c), which is a standardized index based on the observed sea level pressure differences between Tahiti and Darwin, Australia. The monthly correlation between SST and T2 is high throughout the study region, most markedly ($R > 0.95$) over all Northwest Pacific. The effect of T2 on SST is significant over 98% of the study region in all seasons. This is in good agreement with the previous studies (Skloris et al, 2012; Shaltout and Omstedt, 2014). Similarly, based on monthly data, there is a significant positive correlation between SST and Total Column Water (TCW), precipitation (PRCP).

380

381

382

The maximum negative correlation between the effect of Wind Speed 10m (WS10) on SST occurs southeast Northwest Pacific, and significant in an only small region. However, the direct correlation between V10 and SST is significant and positive over more of the Northwest Pacific.



384

385

386

Figure 9. The correlation coefficient between SST and the atmospheric components. (level of significance equal to 0.05).

387

3.4. The Near China Sea SST characteristics

388

389

390

391

392

393

394

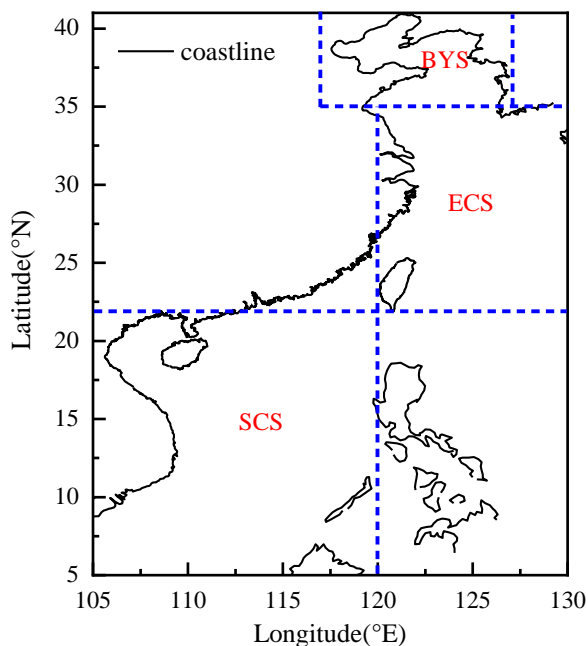
The Near China Sea is defined as the four sea areas of the Bohai Sea, Yellow Sea, East China Sea, and South China Sea, and include the Kuroshio Extension, the part of Northwest Pacific and the sea surrounding Japan in this study, which defined as the offshore region of 5°N-41°N and 105°E-130°E. The changes in the average SST in the Yellow Sea and the Bohai Sea are very similar, so we analyze the two sea areas together. Therefore, the region is further divided into three sub-regions: Bohai Sea and Yellow Sea (BYS, 35°N-41°N and 117°E-127°E), East China Sea (ECS, 22°N-35°N and 120°E-130°E) and South China Sea (SCS, 5°N-22°N and 105°E-120°E)²⁵.

395

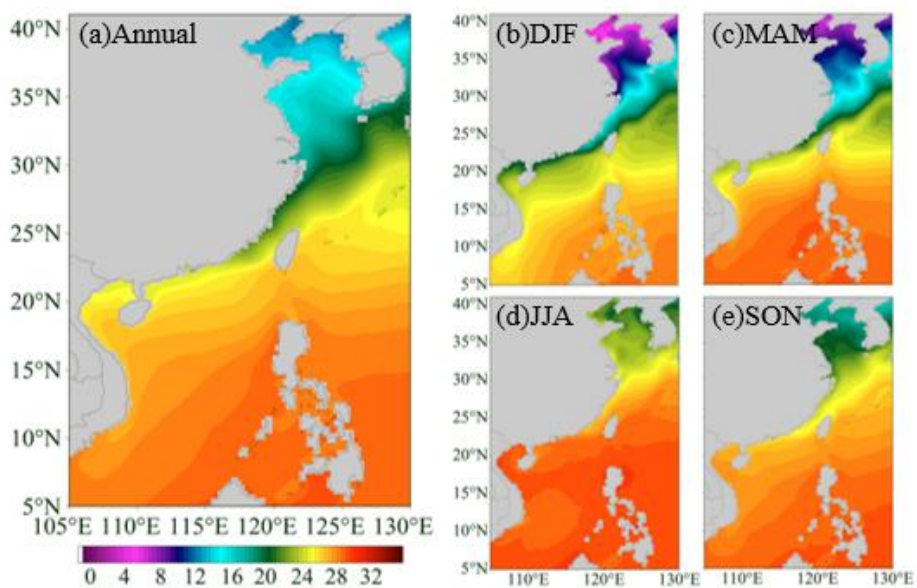
396

Fig.11 shows the spatial distribution of seasonal and annual mean SST in the Near China Sea during the 1988-2017 period. Annual mean SST decreases with increasing latitude, with high temperature ranging

397 from 26°C to 28°C in the south and low temperature ranging from 14°C to 16°C in the north, which is
 398 closely related to the solar radiation distribution in the offshore region. The isotherm is northeast–
 399 southwest oriented and the SST gradient increases as getting closer to the mainland coastal line. It is
 400 obvious that the landmass effect in the winter has contributed to the tilting of the isotherms, which was
 401 pointed out by Bao et al. ²⁵. The ECS exhibits the largest temperature gradient, and the SCS in the tropical
 402 zone the lowest temperature gradient.

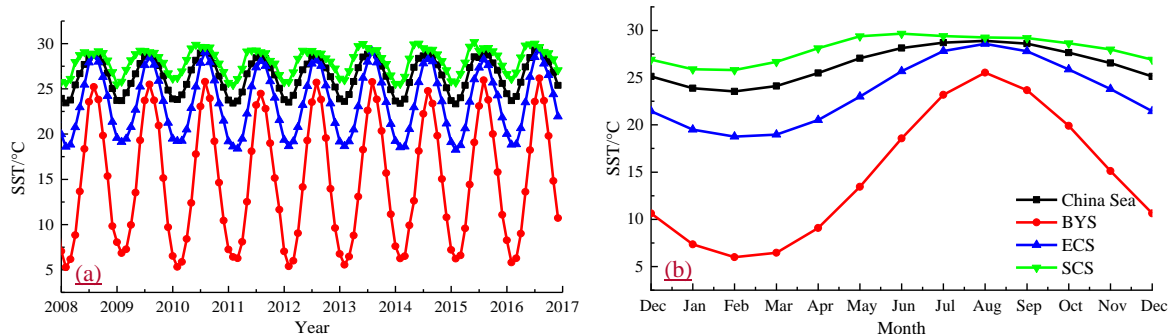


403
 404 **Figure 10.** Study regions defined in this paper. BYS: the Bohai Sea and the Yellow Sea; ECS:
 405 the East China Sea; SCS: the South China Sea.



406
 407 **Figure 11.** Annual (left) and seasonal (right) mean SST distribution during 1988-2017 in the
 408 China Sea. (a) Annual; (b) Winter: DJF; (c) Spring: MAM; (d) Summer: JJA; (e) Autumn: SON.

409 The monthly mean surface temperature changes over the past 10 years in the three regions (BYS,
 410 ECS and SCS) and the whole sea area (China Sea) are shown in Fig. 12. Fig. 12(a) shows the year-by-year
 411 variation of SST in different regions in the last 10 years, and Fig.12(b) shows the monthly SST variations
 412 in different regions in the past 10 years. The change variability of SST in different regions are basically
 413 synchronized. The minimum temperature basically occurs in February and the warmest occurs in August.
 414 The fluctuation range of SST in BYS is the largest, basically between 5 °C to 22 °C, from 18 °C to 27 °C
 415 in the East China Sea, and the smallest fluctuations is in the South China Sea, maintained at a range of
 416 26 °C to 29 °C. There are large differences between the mean and standard deviation in different regions.



417

418 **Figure 12.** Long term monthly mean SST of the marginal seas of China during 2008-2017 (a)
 419 Yearly; (b) Monthly. Black line: China Sea; red line: Bohai Sea and Yellow Sea (BYS); blue
 420 line: East China Sea (ECS); green line: South China Sea (SCS).

421 Table 2 shows the annual and seasonal SST characteristics of the study area Near China Sea based
 422 on monthly data from 1988 to 2017. It can be found that in addition to the winter and spring in the BYS,
 423 the SST in each season of other regions shows an increasing trend from the table. Average increasing
 424 trends of SST during 1988 to 2017 in BYS is 0.015 °C/ 10yr, 0.14 °C/ 10yr for the ECS, 0.12 °C/ 10yr for
 425 the SCS and 0.12 °C/ 10yr for whole Near China Sea respectively, and all the trends are significant at the
 426 99% confidence level. From the point of average annual SST, the SST in the South China Sea is the highest,
 427 reaching 28.01°C, followed by the East China Sea with 23.4°C, the lowest in the Bohai Sea and the Yellow
 428 Sea is 14.98°C, and the SST in the whole Near China Sea is 26.4°C. Table 3 shows the peak value and
 429 time of the annual and seasonal SST of the study area Near China Sea based on monthly data from 1988
 430 to 2017. In the past 30 years, colder SST occurs in 1989, 1990, 1992, 1993, 2003, 2008, 2010, 2011.
 431 Warmer SST occurs in 1997, 1998, 1999, 2001, 2015, 2016.

432

433
434

Table 2. Annual and seasonal SST characteristics of the study area Near China Sea based on monthly data from 1988 to 2017.

	Average trend (°C/10yr)					Average (°C) ± standard deviation				
	Winter	Spring	Summer	Autumn	Annual	Winter	Spring	Summer	Autumn	Annual
BYS	-0.027	-0.097	0.084	0.13	0.015	8.08 ± 0.52	9.84 ± 0.49	22.44 ± 0.54	19.56 ± 0.44	14.98 ± 0.34
ECS	0.11	0.04	0.15	0.23	0.14	19.81 ± 0.33	20.87 ± 0.35	27.24 ± 0.31	25.66 ± 0.34	23.40 ± 0.26
SCS	0.13	0.10	0.11	0.14	0.12	26.09 ± 0.33	28.02 ± 0.27	29.38 ± 0.28	28.54 ± 0.27	28.01 ± 0.23
Whole	0.13	0.08	0.11	0.16	0.12	24.07 ± 0.27	25.53 ± 0.25	28.50 ± 0.24	27.50 ± 0.26	26.40 ± 0.21

435
436

Table 3. Peak value and time of the annual and seasonal SST of the study area Near China Sea based on monthly data from 1988 to 2017.

	Minimum (°C) and time (yr)					Maximum (°C) and time (yr)				
	Winter	Spring	Summer	Autumn	Annual	Winter	Spring	Summer	Autumn	Annual
BYS	7.13 (2003)	8.88 (2010)	21.13 (1993)	18.69 (1992)	14.45 (2010)	9.17 (2001)	11.02 (1998)	23.99 (1997)	20.70 (1998)	15.85 (1998)
ECS	19.30 (1989)	20.04 (2011)	26.76 (1993)	25.01 (1992)	22.97 (1993)	20.54 (1999)	21.84 (1998)	28.06 (2016)	26.43 (1998)	24.14 (1998)
SCS	25.53 (1993)	27.50 (2011)	28.97 (2008)	27.98 (1992)	27.68 (1989)	26.78 (2016)	28.53 (2001)	30.02 (1998)	29.14 (2015)	28.58 (1998)
Whole	23.61 (1993)	24.99 (2011)	28.18 (1990)	26.94 (1992)	26.07 (1993)	24.63 (1999)	26.05 (1998)	29.09 (1998)	28.18 (1998)	26.98 (1998)

437 **4. Conclusions**

438 The Northwest Pacific sea surface variability is affected by a combination of oceanic and atmospheric
439 processes and displays significant regional and seasonal behavior. Monthly SST datasets based on ERSST
440 3b (1854-2017, 164 years) and OISST V2 (1988-2017, 30 years) are used to make some long-term
441 temporal and spatial variability statistics. The following conclusions can be drawn from the analysis.

442 In the last 164 years, SST in the Northwest has gradually increased, with an increasing trend of
443 0.033 °C/10 yr. Especially in the past 30 years, the increasing trend of SST reaches to 0.132 °C/10 yr, and
444 the increasing trend of SST reaches to 0.306 °C/10 yr in the last 10 years, which increasing trend is very
445 obviously. The trend of the SST varies seasonally. The increasing trend in winter and autumn are
446 0.124 °C/10 yr and 0.146 °C/10 yr respectively, which are greater than spring and summer, with
447 0.075 °C/10 yr and 0.107°C /10 yr respectively. There was an SST extremum point occurred
448 around 1998, the average annual SST for the 10 years after 1998 increased by 0.3°C over the previous 10
449 years. It has been found that the change of SST/SSTA in the Northwest Pacific is closely related to the
450 ENSO through the statistical analysis of Nino3.4 index and SST/SSTA.

451 From the perspective of spatial distribution, the annual mean SST decreases with increasing latitude
452 in conclusion, with high temperature ranging from 27°C to 33°C in the south and low temperature ranging
453 from 3°C to 15°C in the north. The SST is higher in the low-latitude (near equator) region and lower in
454 the high-latitude region. In the low-latitude region, SST is more evenly distributed along the latitudes in
455 November to April, but from May to October, the distribution of SST along the latitude is tilted, showing
456 the distribution characteristics of higher in the southwest and lower in the northeast, which is affected by
457 the ocean circulation.

458 There are many correlations between the SST and some climate indexes and atmospheric parameters,
459 such as Pacific Decadal Oscillation (PDO), Southern Oscillation Index (SOI), Nino 3.4, total water vapor
460 column (TWC), temperature at 2 meters (T2), sea level pressure (SLP), precipitation (PRCP) and wind
461 speed at 10 meters (U10, V10 and WS10). A very significant positive correlation between SST and T2,
462 TCW was been found, of which the correlation coefficient between SST and T2 exceeded 98%. PDO,
463 Nino 3.4 is negatively correlated with SST, and the correlation between other indexes and parameters and
464 SST is weak.

465 The whole Near China Sea was divided into three sections to analysis its spatial variability in a
466 different region, which is the Bohai Sea and Yellow Sea (BYS), East China Sea (ECS) and South China
467 Sea (SCS). The SST in the BYS is coolest with a range from 5 °C to 22 °C, and the warmest in the SCS
468 with a range from 26 °C to 29 °C. It can be seen from the statistical data that in addition to the winter and
469 spring in the BYS, SST in other regions and time had shown a warming trend. In the past 30 years, the
470 trend of SST increase of BYS was 0.015 °C/10 yr, while that of ECS and SCS was 0.14 °C/10 yr and
471 0.12 °C/10 yr, respectively.

472 **Competing interests:** The authors declare that they have no conflict of interest.

473 **Financial support:** The study was supported by the National Natural Science Foundation of China
474 (Grant Nos. 51809023, 51839002 and 51879015).

475 **References:**

- 476 Ault, T. R., Cole, J. E., Evans, M. N., Barnett, H., Abram, N. J., Tudhope, A. W., and Linsley., B. K.:
477 Intensified decadal variability in tropical climate during the late 19th century, *Geophysical Research*
478 *Letters*, 36, L08602, <https://doi.org/10.1029/2008GL036924>, 2009.
- 479 Bao, B., and Ren, G.: Climatological characteristics and long-term change of SST over the marginal seas
480 of China, *Continental Shelf Research*, 77, 96-106, <https://doi.org/10.1016/j.csr.2014.01.013>, 2014.
- 481 Buckley, M. W., Ponte, R. M., Forget, G., and Heimbach, P.: Low-frequency SST and upper-ocean heat
482 content variability in the North Atlantic, *Journal of Climate*, 27, 4996-5018,
483 <https://doi.org/10.1175/JCLI-D-13-00316.1>, 2014.
- 484 Chelton, D. B., and Xie, S. P.: Coupled ocean-atmosphere interaction at oceanic mesoscales,
485 *Oceanography*, 23, 52-69, <https://doi.org/10.5670/oceanog.2010.05>, 2010.

486 Chen, Z., Wen, Z., Wu, R., Lin, X., and Wang, J.: Relative importance of tropical SST anomalies in
487 maintaining the Western North Pacific anomalous anticyclone during El Niño to La Niña transition
488 years, *Climate dynamics*, 46, 1027-1041, <https://doi.org/10.1007/s00382-015-2630-1>, 2016.

489 Diamond, M. S., and Bennartz, R.: Occurrence and trends of eastern and central Pacific El Niño in different
490 reconstructed SST data sets, *Geophysical Research Letters*, 42, 10375–10381,
491 <https://doi.org/10.1002/2015GL066469>, 2015.

492 England, M. H., McGregor, S., Spence, P., Meehl, G. A., Timmermann A., Cai W., Gupta A. S., McPhaden
493 M. J., Purich A., and Santoso A.: Recent intensification of wind-driven circulation in the Pacific and
494 the ongoing warming hiatus, *Nature Climate Change*, 4, 222, <https://doi.org/10.1038/nclimate2106>,
495 2014.

496 Franch, B., Vermote, E.F., Roger, J.-C., Murphy, E., Becker-Reshef, I., Justice, C., Claverie, M., Nagol,
497 J., Csizsar, I., Meyer, D., Baret, F., Masuoka, E., Wolfe, R., and Devadiga, S.: A 30+ Year AVHRR
498 Land Surface Reflectance Climate Data Record and Its Application to Wheat Yield Monitoring,
499 *Remote Sensing*, 9, 296, <https://doi.org/10.3390/rs9030296>, 2017.

500 Gergis, J. L., and Fowler, A. M.: Classification of synchronous oceanic and atmospheric El Niño-Southern
501 Oscillation (ENSO) events for palaeoclimate reconstruction, *International Journal of Climatology*,
502 25, 1541-1565, <https://doi.org/10.1002/joc.1202>, 2005.

503 Graham, N. E.: Decadal-scale climate variability in the tropical and North Pacific during the 1970s and
504 1980s: Observations and model results, *Climate Dynamics*, 10, 135-162,
505 <https://doi.org/10.1007/BF00210626>, 1994.

506 Griffies, S. M., Winton, M., Anderson, W. G., Benson, R., Delworth, T. L., Dufour, C. O., Dunne, J. P.,
507 Goddard, P., Morrison, A. K., Rosati, A., Wittenberg, A. T., Yin, J., and Zhang R.: Impacts on ocean
508 heat from transient mesoscale eddies in a hierarchy of climate models, *Journal of Climate*, 28, 952-
509 977, <https://doi.org/10.1175/JCLI-D-14-00353.1>, 2015.

510 Hu, H., Wu, Q., and Wu, Z.: Influences of two types of El Niño event on the Northwest Pacific and tropical
511 Indian Ocean SST anomalies, *Journal of Oceanology and Limnology*, 36, 33-47,
512 <https://doi.org/10.1007/s00343-018-6296-5>, 2018.

513 Huang, B., Banzon, V. F., Freeman, E., Lawrimore, J., Liu, W., Peterson, T. C., Smith, T. M., Thorne, P.
514 W., Woodruff S. D., and Zhang, H. M.: Extended reconstructed sea surface temperature version 4
515 (ERSST. v4). Part I: upgrades and intercomparisons, *Journal of climate*, 28, 911-930,
516 <https://doi.org/10.1175/JCLI-D-14-00006.1>, 2015.

517 Huang, B., Thorne, P. W., Smith, T. M., Liu, W., Lawrimore, J., Banzon, V. F., and Menne, M. Further
518 exploring and quantifying uncertainties for extended reconstructed sea surface temperature (ERSST)
519 version 4 (v4), *Journal of Climate*, 29, 3119-3142, <https://doi.org/10.1175/JCLI-D-15-0430.1>, 2016.

520 Kosaka, Y., and Xie, S. P.: Recent global-warming hiatus tied to equatorial Pacific surface cooling, *Nature*,
521 501, 403, <https://doi.org/10.1038/nature12534>, 2013.

522 Latif, M.: On North Pacific multidecadal climate variability, *Journal of climate*, 19, 2906-2915,
523 <https://doi.org/10.1175/JCLI3719.1>, 2006.

524 Li, G., Li, C., Tan, Y., and Bai, T. The interdecadal changes of south pacific sea surface temperature in
525 the mid-1990s and their connections with ENSO, *Advances in Atmospheric Sciences*, 31, 66-84,
526 <https://doi.org/10.1007/s00376-013-2280-3>, 2014.

527 Li, X., Zong, Y., Zheng, Z., Huang, G., and Xiong, H.: Marine deposition and sea surface temperature
528 changes during the last and present interglacials in the west coast of Taiwan Strait, *Quaternary*
529 *International*, 440, 91-101, <https://doi.org/10.1016/j.quaint.2016.05.023>, 2017.

530 Liu, C., Sun, Q., Xing, Q., Liang, Z., Deng, Y., and Zhu, L.: Spatio-temporal variability in sea surface
531 temperatures for the Yellow Sea based on MODIS dataset, *Ocean Science Journal*, 52, 1-10,
532 <https://doi.org/10.1007/s12601-017-0006-7>, 2017.

533 McCarthy, G. D., Haigh, I. D., Hirschi, J. J. M., Grist, J. P., and Smeed, D. A.: Ocean impact on decadal
534 Atlantic climate variability revealed by sea-level observations, *Nature*, 521, 508,
535 <https://doi.org/10.1038/nature14491>, 2015.

536 Mei, W., Xie, S. P., Primeau, F., McWilliams, J. C., and Pasquero, C.: Northwestern Pacific typhoon
537 intensity controlled by changes in ocean temperatures, *Science Advances*, 1, e1500014,
538 <https://doi.org/10.1126/sciadv.1500014>, 2015.

539 Pachauri, R. K., Allen, M. R., Barros, V. R., Broome, J., Cramer, W., Christ, R., Church, J. A., Clarke, L.,
540 Dahe, Q., Dasgupta, P., Dubash, N. K., et al.: *Climate Change 2014: Synthesis Report. Contribution*
541 *of Working Groups I, II and III to the Fifth Assessment Report of the Intergovernmental Panel on*
542 *Climate Change / R. Pachauri and L. Meyer (editors)*, Geneva, Switzerland, IPCC, ISBN: 978-92-
543 9169-143-2, 2014.

544 Pan, X., Wong, G. T., Ho, T. Y., Tai, J. H., Liu, H., Liu, J., and Shiah, F. K.: Remote sensing of surface
545 [nitrite+ nitrate] in river-influenced shelf-seas: The northern South China Sea Shelf-sea, *Remote*
546 *Sensing of Environment*, 210, 1-11, <https://doi.org/10.1016/j.rse.2018.03.012>, 2018.

547 Reynolds, R. W., Rayner, N. A., Smith, T. M., Stokes, D. C., and Wang, W.: An improved in situ and
548 satellite SST analysis for climate, *Journal of climate*, 15: 1609-1625, [https://doi.org/10.1175/1520-](https://doi.org/10.1175/1520-0442(2002)015)
549 [0442\(2002\)015](https://doi.org/10.1175/1520-0442(2002)015), 2002.

550 Reynolds, R. W., Smith, T. M., Liu, C., Chelton, D. B., Casey, K. S., and Schlax, M. G.: Daily high-
551 resolution-blended analyses for sea surface temperature, *Journal of Climate*, 20, 5473-5496,
552 <https://doi.org/10.1175/2007JCLI1824.1>, 2007.

553 Robinson, C. J.: Evolution of the 2014–2015 sea surface temperature warming in the central west coast of
554 Baja California, Mexico, recorded by remote sensing, *Geophysical Research Letters*, 43, 7066-7071,
555 <https://doi.org/10.1002/2016GL069356>, 2016.

556 Shakun, J. D., and Shaman, J.: Tropical origins of North and South Pacific decadal variability, *Geophysical*
557 *Research Letters*, 36, L19711, <https://doi.org/10.1029/2009GL040313>, 2009,

558 Shaltout, M., and Omstedt, A.: Recent sea surface temperature trends and future scenarios for the
559 Mediterranean Sea, *Oceanologia*, 56, 411-443, <https://doi.org/10.5697/oc.56-3.411>, 2014.

560 Skirving, W., Enríquez, S., Hedley, J.D., Dove, S., Eakin, C.M., Mason, R.A.B., De La Cour, J.L., Liu,
561 G., Hoegh-Guldberg, O., Strong, A.E., Mumby, P.J., and Iglesias-Prieto, R.: Remote Sensing of Coral

562 Bleaching Using Temperature and Light: Progress towards an Operational Algorithm, *Remote*
563 *Sensing*, 10, 18, <https://doi.org/10.3390/rs10010018>, 2018.

564 Skliris, N., Sofianos, S., Gkanasos, A., Mantziafou, A., Vervatis, V., Axaopoulos, P., and Lascaratos, A.:
565 Decadal scale variability of sea surface temperature in the Mediterranean Sea in relation to
566 atmospheric variability, *Ocean Dynamics*, 62, 13-30, <https://doi.org/10.1007/s10236-011-0493-5>,
567 2012.

568 Smith, C. A., Compo, G. P., and Hooper, D. K.: Web-Based Reanalysis Intercomparison Tools (WRIT)
569 for analysis and comparison of reanalyses and other datasets, *Bulletin of the American*
570 *Meteorological Society*, 95, 1671-1678, <https://doi.org/10.1175/BAMS-D-13-00192.1>, 2014.

571 Smith, T. M., Reynolds, R. W., Peterson, T. C., and Lawrimore, J.: Improvements to NOAA's historical
572 merged land-ocean surface temperature analysis (1880–2006), *Journal of Climate*, 21, 2283-2296,
573 <https://doi.org/10.1175/2007JCLI2100.1>, 2008.

574 Stuecker, M. F., Jin, F. F., Timmermann, A., and McGregor, S. Combination mode dynamics of the
575 anomalous northwest Pacific anticyclone, *Journal of Climate*, 28, 1093-1111,
576 <https://doi.org/10.1175/JCLI-D-14-00225.1>, 2015.

577 Song, D., Duan, Z., Zhai, F., and He, Q.: Surface diurnal warming in the East China Sea derived from
578 satellite remote sensing, *Chinese Journal of Oceanology and Limnology*, 36, 620–629,
579 <https://doi.org/10.1007/s00343-018-7035-7>, 2018.

580 Takakura, T., Kawamura, R., Kawano, T., Ichiyanagi, K., Tanoue, M., and Yoshimura, K.: An estimation
581 of water origins in the vicinity of a tropical cyclone's center and associated dynamic processes,
582 *Climate Dynamics*, 50, 555-569, <https://doi.org/10.1007/s00382-017-3626-9>, 2018.

583 Tang, D., Kester, D. R., Wang, Z., Lian, J., and Kawamura, H. AVHRR satellite remote sensing and
584 shipboard measurements of the thermal plume from the Daya Bay, nuclear power station, China,
585 *Remote Sensing of Environment*, 84, 506-515, [https://doi.org/10.1016/S0034-4257\(02\)00149-9](https://doi.org/10.1016/S0034-4257(02)00149-9),
586 2003.

587 Tian, F., von Storch, J. S., and Hertwig, E.: Impact of SST diurnal cycle on ENSO asymmetry[J]. *Climate*
588 *Dynamics*, 52, 2399–2411, <https://doi.org/10.1007/s00382-018-4271-7>, 2019.

589 Trenberth, K. E., and Hurrell, J. W.: Decadal atmosphere-ocean variations in the Pacific, *Climate*
590 *Dynamics*, 9, 303-319, <https://doi.org/10.1007/BF00204745>, 1994.

591 Wang, C., Zou, L., and Zhou, T.: SST biases over the Northwest Pacific and possible causes in CMIP5
592 models, *Science China Earth Sciences*, 61, 1-12, <https://doi.org/10.1007/s11430-017-9171-8>, 2018.

593 Wang, Y., Liu, P., Li, T., and Fu, Y.: Climatologic comparison of HadISST1 and TMI sea surface
594 temperature datasets, *Science China Earth Sciences*, 54, 1238-1247, <https://doi.org/10.1007/s11430-011-4214-1>, 2011.

596 Wills, R. C., Schneider, T., Wallace, J. M., Battisti, D. S., and Hartmann, D. L.: Disentangling global
597 warming, multidecadal variability, and El Niño in Pacific temperatures, *Geophysical Research*
598 *Letters*, 45, 2487-2496, <https://doi.org/10.1002/2017GL076327>, 2018.

599 Wu, Z., Jiang, C., Deng, B., Chen, J., Long, Y., Qu, K., and Liu, X.: Simulation of Typhoon Kai-tak using
600 a mesoscale coupled WRF-ROMS model, *Ocean Engineering*, 175, 1-15,
601 <https://doi.org/10.1016/j.oceaneng.2019.01.053>, 2019a.

602 Wu Z, Jiang C, Deng B, et al. Sensitivity of WRF simulated typhoon track and intensity over the South
603 China Sea to horizontal and vertical resolutions, *Acta Oceanologica Sinica*, 38(7): 74-83,
604 <https://doi.org/10.1007/s13131-019-1459-z>, 2019b.

605 Wu, Z., Jiang, C., Chen, J., Long, Y., Deng, B., and Liu, X.: Three-Dimensional Temperature Field Change
606 in the South China Sea during Typhoon Kai-Tak (1213) Based on a Fully Coupled Atmosphere–
607 Wave–Ocean Model, *Water*, 11, 140, <https://doi.org/10.3390/w11010140>, 2019c.

608 Wu, Z., Jiang, C., Conde, M., Deng, B., and Chen, J.: Hybrid improved empirical mode decomposition
609 and BP neural network model for the prediction of sea surface temperature, *Ocean Science*, 15, 349-
610 360, <https://doi.org/10.5194/os-15-349-2019>, 2019d.

611 Xiao, M., Zhang, Q., and Singh, V. P.: Influences of ENSO, NAO, IOD and PDO on seasonal precipitation
612 regimes in the Yangtze River basin, China, *International Journal of Climatology*, 35, 3556-3567,
613 <https://doi.org/10.1002/joc.4228>, 2015.

614 Xu, L., He, S., Li, F., Ma, J., and Wang, H. Numerical simulation on the southern flood and northern
615 drought in summer 2014 over Eastern China, *Theoretical and Applied Climatology*, 134, 1-13,
616 <https://doi.org/10.1007/s00704-017-2341-0>, 2018.

617 Xue, X., Chen, W., Chen, S., and Feng, J.: PDO modulation of the ENSO impact on the summer South
618 Asian high, *Climate Dynamics*, 50, 1393-1411, <https://doi.org/10.1007/s00382-017-3692-z>, 2018.

619 Yamamoto, R., Iwashima, T., and Hoshiai, M.: An analysis of climatic jump, *Journal of the Meteorological*
620 *Society of Japan. Ser. II*, 64, 273-281, https://doi.org/10.2151/jmsj1965.64.2_273, 1986.

621 Yang, L., Chen, S., Wang, C., Wang, D., and Wang, X.: Potential impact of the Pacific Decadal Oscillation
622 and sea surface temperature in the tropical Indian Ocean–Western Pacific on the variability of
623 typhoon landfall on the China coast, *Climate Dynamics*, 51, 1-11, <https://doi.org/10.1007/s00382-017-4037-7>, 2017.

624

625 Yang, J., Gong, P., Fu, R., Zhang, M., Chen, J., Liang, S., Xu, B., Shi, J., and Dickinson, R.: The role of
626 satellite remote sensing in climate change studies, *Nature climate change*, 3, 875,
627 <https://doi.org/10.1038/nclimate1908>, 2013.

628 Zhang, C., Li, H., Liu, S., Shao, L., Zhao, Z., and Liu, H.: Automatic detection of oceanic eddies in
629 reanalyzed SST images and its application in the East China Sea, *Science China Earth Sciences*, 58,
630 2249-2259, <https://doi.org/10.1007/s11430-015-5101-y>, 2015.

631 Zheng, X. T., Xie, S. P., Lv, L. H., and Zhou, Z. Q.: Intermodel uncertainty in ENSO amplitude change
632 tied to Pacific Ocean warming pattern, *Journal of Climate*, 29, 7265-7279,
633 <https://doi.org/10.1175/JCLI-D-16-0039.1>, 2016.

634 Zhou, T., Yu, R., Zhang, J., Drange, H., Cassou, C., Deser, C., Hodson, D. L. R., Sanchez-Gomez E., Li, J.,
635 Keenlyside, N., Xin, X., and Okumura, Y.: Why the western Pacific subtropical high has extended
636 westward since the late 1970s, *Journal of Climate*, 22, 2199-2215,
637 <https://doi.org/10.1175/2008JCLI2527.1>, 2009.